EXOMARS ROVER CHASSIS ANALYSIS & DESIGN

Alex Ellery[(1)], Nildeep Patel[(1)], Lutz Richter[(2)], Reinhold Bertrand[(3)], Josef Dalcomo[(3)]

[(1)] *Surrey Space Centre, University of Surrey, Guildford, GU2 7XH, UK: a.ellery@surrey.ac.uk, nil.patel@surrey.ac.uk*
[(2)] *Deutschen Zentrum fur Luft und Raumfahrt (DLR), Institute of Space Simulation, Linder Hoehe D-51170, Koln, Germany: lutz.richter@dlr.de*
[(3)] *von Hoerner & Sulger GmbH, D-68723 Schwetzingen, Germany: mail@bertrand.de, dalcolmo@vh-s.de*

ABSTRACT

The European ExoMars mission represents the first flagship of the European ExoMars programme for the robotic exploration of Mars. The ambitious rover of 200+kg carries the 40 kg Pasteur scientific instrument suite to conduct exobiology-focussed investigation of the Martian surface and near sub-surface. The rover is required to be highly mobile across a potentially hostile terrain. This mobility is the key to maximising the availability of potential sites of scientific interest. Hence, the chassis design is critical in determining the effectiveness of achievability of its scientific targets. The chassis design and its tractive performance is the focus of this paper.

1. INTRODUCTION

The European ExoMars mission represents the first flagship of the Aurora programme. Aurora represents a staged programme of missions culminating in the safe landing and return of humans to Mars around 2030. The first flagship, ExoMars, is a robotic exploration mission centred on a large rover of ~200+kg carrying a scientific instrument suite (Pasteur) of around 40 kg to carry out exobiology-focussed investigation of the Martian surface and near sub-surface. This includes a subsurface drilling system supported by a sample handling system. This ambitious mission imposes considerable challenges. From a scientific point of view, the exobiology focus is unique as no other mission to Mars has explored the potential for exobiology since the Viking landers over 20 years ago. Exobiology in particular requires a diverse instrument suite and analytical handling capabilities. However, it particularly imposes considerable requirements on the mobility requirements – exobiological sampling is by its nature discrete and requires multiple sampling sites. Thus far, two US rovers have been deployed on Mars – the Sojourner micro-rover and the two Mars Exploration Rovers, Spirit and Opportunity. The mobility issue was reinforced by Opportunity which was close to Opportunity Ledge of high scientific interest – a lack of mobility would have represented a significant lost opportunity for such high scientific return. Indeed, it may be concluded that the day of the static lander without a rover element has passed. This requirement for high mobility is contrasted by the hostility of the Martian terrain. The ExoMars chassis must be robust with minimal mass and complexity overhead. Yet the chassis is the key to maximising the availability of potential sites of scientific interest, and so, maximising the scientific return of the mission. The rover must operate in a wide variety of conditions. Furthermore, the chassis design has considerable impact on the approaches to autonomous navigation that may be required. Although the ExoMars landing site has yet to be selected (which has a strong impact on such issues as power generation and thermal control), we have utilised previous Mars mission data (rock distribution and soil parameters) to provide realistic performance estimates of different rover chassis designs. Several of the chassis designs were proposed by VNIITransmash Russia. The chassis selection criteria were complex and included traditional vehicle performance metrics, tractive performance modelling, 3D modelling, mean free path analysis as well as constraints such as mass impact, complexity, maturity and heritage. This paper outlines the process of these analyses, the chassis selection decision-making and their rationale, particularly with regard to traction performance.

2. OVERVIEW OF THE EXOMARS ROVER

The primary objectives of the ExoMars rover were to seek signs of extant or extinct life on Mars and to identify potential hazards to human exploration. The ExoMars rover comprises three major subsystems: the Pasteur payload, the rover service module and the rover chassis (Fig 1). The primary constraints on the ExoMars rover design are mass, energy,

and time. The rover has limited communications with Earth so must employ considerable levels of onboard autonomy without ground intervention (CCSDS Proximity-1 space link protocol) – it must be able to operate nominally for 48 hours and survive in recoverable safe mode for 30 sols. ExoMars will use UHF capable of up to 2048 kbps return data rates for communicating with an orbiter in a store-and-forward protocol with the option for an X-band direct-to-Earth communications system – indeed, MERs relayed the vast majority of its data through the MGS/Odyssey orbiter relays. Less than one communication window per day was envisaged for uploading from the ground. The high volume of scientific data particularly due to images, wavelet compression is adopted for storage and transmission (600 kB per colour image) to enable storage for 48 hours. The communications cycle was expected to transmit 550 Mb of data. The Pasteur payload nominally includes: a multi-spectral panoramic stereo-camera pair and high resolution imager, an multi-sensor environment package (similar to Beagle 2), an optical colour microscope, a combined visible laser Raman spectrometer/laser induced breakdown spectrometer, a combined gas chromatograph/mass spectrometer, a life marker chip, an oxidant sensor, and optionally a subsurface electromagnetic sounder. It includes a multi-rod drill to collect soil samples to a depth of 1.5+ m (estimates of the average depth of the Martian regolith are around 10m, the upper few metres which have been vertically mixed by impact gardening) and core surface rocks to a depth of 30 mm, and a sample handling system for sample powdering and polishing. Experiments are controlled through time-tagged execution of pre-stored activity sequences (modifiable by telecommand). Autonomous onboard power scheduling is also required. Solar power availability was designed account for 0.3% per day degradation of solar arrays due to dust deposition. Energy storage is through rechargeable Li ion batteries. The thermal control of the rover is particularly challenging as a narrow temperature of –10 to 20^{o} C is required for the payload particularly during the night – this necessitates 30-50 mm of insulation unless aerogel is adopted. The ExoMars rover is perceived to hibernate during the night to minimise power consumption and power storage requirements with energy supplied by RHUs to maintain thermal requirements to minimise battery capacity requirements.

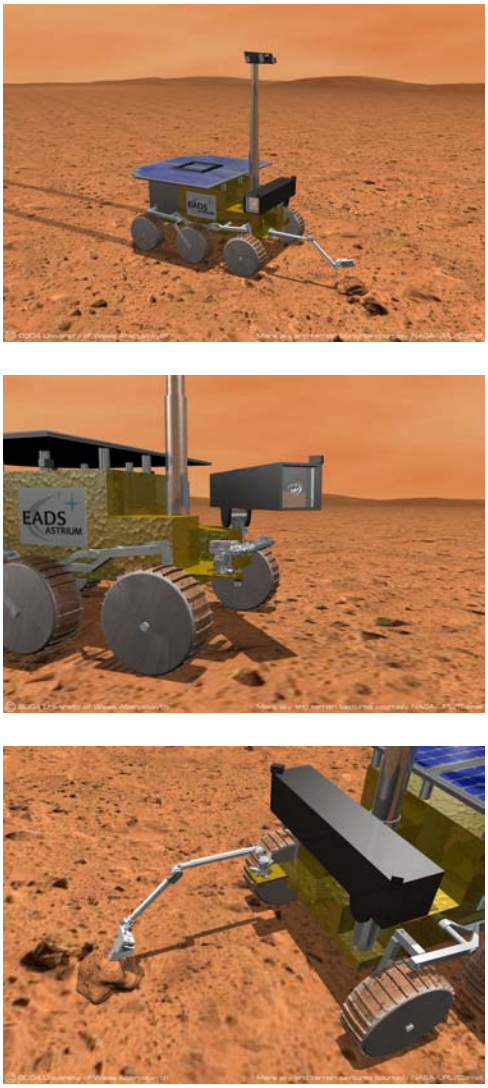

Fig 1. ExoMars rover (a) overall view; (b) drill deployment; (c) arm deployment (from EADS Astrium)

3. EXOMARS OPERATIONAL MISSION

The ExoMars rover and chassis were designed to withstand landing loads of 120g. On safe landing and checkout, the rover is deployed from its stowed configuration on a baseplate within the lander to its nominal configuration and deployed down a ramp. Chassis deployment was based on six motorised mechanisms – rotating the front and rear wheels outwards and downwards in opposing directions (230^{o} rotation angle), and the middle wheels deployed in either direction (180^{o} rotation angle). Each motor (six drive motors and four corner steering motors) were considered to include planetary gearboxes, the complete assembly sealed with dry lubricant slide bearings to protect from dust contamination. The operational activities of the ExoMars rover is generally cyclic involving

interleaving the experiment cycle of 6 days, the traversal cycle of 5 days and the communications cycle. The nominal mission shall perform a minimum of 10 experiment cycles up to 20 such cycles for an extended mission. The rover must be able to travel up to 2 km between sampling locations (nominally 0.5 km plus 50% margin of 0.75 km). The nominal average speed of the ExoMars rover traverse was taken to be 100m/day (as for the Mars Exploration Rovers) but MER demonstrated that drive distances per command were limited to 10m. Given that the 100m/day includes hazard avoidance and obstacle negotiation, this translates as 72 m/h (2 cm/s) actual traversal speeds for the purposes of assessing mobility performance.

The rover possesses a pan-tilt stereo navigation camera and a separate scientific panoramic camera as part of Pasteur payload. The requirement for 0.3 mrad/pixel gives a field of view of 18^o for a 1024x1024 pixel camera. The navcam is to be mounted 1.5+m from the ground to give goal tracking of 100m with 1m resolution. The general procedure for navigation is to stop, acquire and process images, navigate for a given distance, and repeat. Continuous imaging, navigating and traversing requires substantial computational resources that are unlikely to be available. With MER, each traverse segment between image captures for self-localisation and obstacle detection was around 30 cm corresponding to an average speed of 35 m/h (though the look-ahead viewing distance is 20 m with a resolution of 10 cm for effective obstacle avoidance). The rover utilised the Unionics central with distributed processor architecture with a maximum processing speed of 30 MHz (the MERs used the RAD6000 with a 25 MHz processor speed). The stereovision algorithms dominated the processing loads during navigation phases of the mission. The navigation control architecture has three hierarchical levels (developed at LAAS France): the functional level includes all basic inbuilt rover servo-level actions as modules with a characteristic feedback cycle of 10-100 Hz; the executive level coordinates the execution of functions by organising their sequencing – it is reactive in nature; the decision level produces the task plan and is based on symbol manipulation with a characteristic feedback cycle of 0.1-10 s.

4. EXOMARS CONFIGURATION & OBSTACLE AVOIDANCE

Obstacle traversal over up to 0.3m obstacles necessitated a ground clearance of 0.31 m and a wheel diameter of 0.35 m (including grousers of height 1 cm) assuming that the chassis may accommodate obstacles up to 1.5 times the wheel diameter (with 50% margin). The wheel is assumed to be essentially rigid rather than elastic. The wheelbase of 0.85m and wheel width of 0.1m were determined by the stowage envelope within the descent module. Static stability was required to be maintained up to terrain inclinations of 40^o in all directions (though a tilt angle exceeding 30^o would invoke hazard alarm). The chassis was required to implement body posture averaging. This limited the height of the ExoMars rover centre of mass to 0.5m maximum from the ground. An earlier, simpler analysis is given here (based on uniform mass distribution within the rover cab and assuming symmetry – see Fig 2):

$$\theta_{\max} = \tan^{-1}\left(\frac{Y_{CG}}{Z_{CG}}\right) = 59^o \quad (1)$$

for up/downhill stability

$$\theta_{\max} = \tan^{-1}\left(\frac{Y_{CG}}{Z_{CG}}\right) = 76^o \quad (2)$$

for crosshill stability

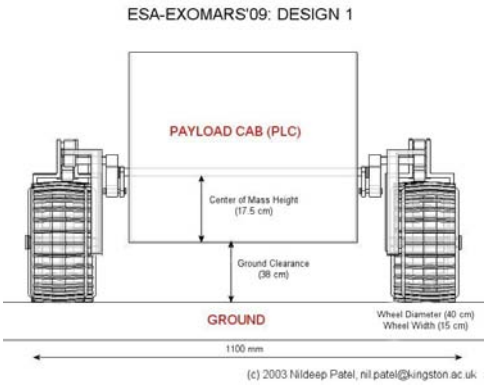

Fig. 2. ExoMars rover chassis configuration for static stability analysis

The mean free path is defined as the expected straight line path distance that a vehicle of a given dimensions can traverse before a heading change is required due to the incidence of an insurmountable obstacle – it provides a metric for manoeuvrability and the requirements for onboard autonomy. The manoeuvrability requirements for the ExoMars rover were that its should be able to traverse rough terrain with the following obstacle distribution:

(i) 1% of area covered with rocks exceeding 0.5m height

(ii) 10% of area covered with rocks exceeding 0.2m height

(iii) 20% of area covered with rocks exceeding 0.005m height

(iv) 1% of area covered with crevasses exceeding 0.25m width and depth

We adopted the Viking Lander 2 (VL2) site as offering the most stringent rock distribution among the known Mars landing sites – it is rockier than 95% of the Martian surface. The frequency of rock coverage for VL2 above a diameter D may be modelled statistically by [1]:

$$\rho(D) = Ke^{-qD} \quad (3)$$

where K_{VL2}=0.176=cumulative fractional area covered by rocks exceeding diameter D
q_{VL2}=2.73
D=minimum rock diameter

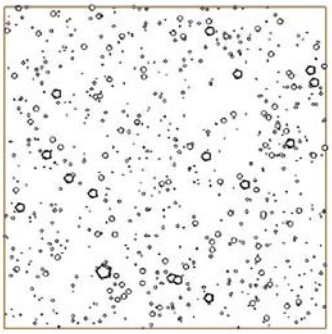

Fig. 3. Randomly-generated Viking lander 2 rock distribution according to rock diameter

This gives 4.5% coverage for condition (i), 10.2% coverage for condition (ii) and 17.4% coverage for condition (iii) (Fig 2). Any rocks of height greater than the rock-climbing ability of the rover will potentially yield a hang-up failure (HUF) depending on the rover chassis kinematic configuration. Condition (iv) may be assumed to be less than equivalent rock coverage of equivalent size if they are vacated locations left by formerly resident boulders – such conditions can yield nose-in failure (NIF) but protrusion of the wheels beyond the front/back of the payload cab avoids this. This condition (iv) is less stringent than the obstacle avoidance conditions so is not examined further. The relevant rock size defined as an obstacle is defined as that which exceeds the maximum vertical height traversable. This is required to be 0.3 m rock height and is determined by the chassis suspension system design – this is assessed through multi-body dynamics modelling using Cosmos-Motion™ software based on the ADAMS™ kernel.

During obstacle traversal, the friction coefficient between metallic wheel and rock is estimated at 0.5. Given that the rocks are embedded within the soil, their heights are related to diameter by [1]:

$$H = 0.506D + 0.008 \quad (4)$$

This assumes that the rock height is approximately half the rock diameter. The mean free path may now be computed as [2,3]:

$$MFP = \frac{1-(r/2)\int_{D_0}^{\infty} D\rho(D)dD - (1/2)\int_{D_0}^{\infty} D^2\rho(D)dD}{r\int_{D_0}^{\infty}\rho(d)dD + \int_{d_0}^{\infty} D\rho(D)dD} \quad (5)$$

where r=vehicle turning diameter

On-the-spot turning was required which may be implemented through skid steering with back-driveable wheel motors (this makes trajectory planning more straightforward). In this case, the vehicle turning diameter is determined by the vehicle diagonal $r = \sqrt{l^2 + w^2}$ - for ExoMars of 1.0m length and 1.2m wheelbase, we obtain a mean free path of 29.6m, ie. 19 obstacles between experiment cycles (for a nominal 500m traverse). However, Ackermann steering was implemented with a turning angle of 30° which yields a 3m turning diameter, reducing the mean free path to 18.7m, yielding 27 such obstacles by virtue of the larger turn diameter. This implies that significant onboard intelligence will be required. Even this may be locally conservative – Sojourner experienced severe difficulties in traversing a local "rock garden" which had a localised areal rock coverage of 24.6% of rocks over 3cm in height.

5. EXOMARS TRACTION PERFORMANCE

The traction performance of planetary rovers is determined by thrust available from the soil and the resistance to motion (such as sinkage), both of which are determined by the nature of the soil and the configuration of the vehicle. In particular, the ground footprint of the vehicle is the determining vehicle characteristic which explains why mean maximum pressure (MMP) is often used as a primitive metric to assess vehicle performance (MMP must not exceed the soil's bearing strength) [4]:

$$MMP_{wheel} = \frac{KW}{2nb^{0.85}d^{1.15}(\delta/h)^{0.5}} \quad (6)$$

where W=vehicle weight (with g=3.73 m/s^2)
n=number of axles
d=wheel diameter
b=wheel width
δ/h=fractional radial tyre deflection
K= parameter defined by proportion of axles driven (all axles for ExoMars)

Thus, traction analysis is essentially independent of chassis suspension. The tractive requirements included being able to traverse 2m long slopes of up to 25^o inclinations on cloddy soils and 18^o inclinations on drift soils. Soil physical properties are defined by the Mohr-Coulomb relation:

$$\tau = C_0 + \sigma \tan\phi \quad (7)$$

where τ=soil shear strength
C_0=cohesive strength of soil (related to cementation)
μ=soil coefficient of friction=tanϕ
ϕ=soil internal angle of friction
σ=normal stress

Sandy soil which is generally characteristic of that found on Mars is defined as soil with low cohesion but high friction [5]. Such soils favour wheeled vehicles which exploit friction rather than tracks which exploit cohesion. Viking lander data indicates higher cohesion than Pathfinder lander data but Viking lander measurements were based on footpad sinkage and trench-digging to depths of 10 cm compared to Pathfinder measurements based on Sojourner's wheel traction experiments restricted to less than 4 cm depths, indicating that the higher cohesion is due to reduction in porosity fraction with depth. DLR soil simulant B reflects the high cohesion of PL drift soil (similar to terrestrial loam) and the low VL1 drift soil friction. DLR soil simulant A reflects the low cohesion of PL cloddy soil and high friction of PL drift soil).

From the Mohr-Coulomb relation, the maximum tractive thrust available from the soil over the vehicle wheel/soil contact area is given by the Bernstein-Bekker equation [6,7]:

$$H = AC_0 + W\tan\phi \quad (8)$$

where A=ground contact area
W=vehicle weight

More complex versions of this equation exist which incorporate parameters such as grouser size (grousers dramatically increase traction). There are a number of additional factors to be accounted for including slip which reduces traction, varies with slope and is notoriously difficult to model [8-10]. The primary resistance to motion is compaction resistance due to sinkage in the soil (there are additional sources of resistance including bulldozing resistance due to the creation of soil bumps in front of the wheels but these are negligible in comparison to compaction resistance (particularly for narrow wheels) [11]. Compaction resistance is given by:

$$R_c = N\left(\frac{kb}{n+1}\right)z^{n+1} \quad (9)$$

where N=number of wheels
b=wheel width
$k = k_c + bk_\phi$=modulus of soil deformation due to sinkage (soil consistency) (N/m^{n+2})
k_c=modulus of cohesion of soil deformation
k_ϕ=modulus of friction of soil deformation
n=soil deformation exponent where 0<n<1.2

Sinkage is determined from the Bernstein-Goriatchkin relation:

$$z = \left(\frac{W}{A(k/b)}\right)^{1/n} = \left(\frac{p}{k/b}\right)^{1/n} \quad (10)$$

where W=wheel load=pA
p=ground pressure load
A=wheel contact area

Given the absence of actual Martian data on the Martian soil deformation constants, we have adopted lunar soil values [12]:

k=shear deformation slip modulus=0.018 m for the Moon
k_c=modulus of cohesion of soil deformation=0.14 N/cm^2 for the Moon
k_ϕ=modulus of friction of soil deformation=0.82 N/cm^3 for the Moon
n=soil deformation exponent=1.0 (for a Gerstner soil such as sand)

The traction performance metric – drawbar pull – is defined by:

$$DP = H - R \quad (11)$$

where $R = R_c + R_o$

R_c=compaction resistance
R_o=other resistances

The results for the ExoMars rover configuration are defined in Table 1 in terms of drawbar pull and maximum slope angle for a range of different soils indicating that for all soils, the ExoMars rover configuration can provide traction for forward motion:

Soil	Specific gravity (ρg)	Soil Cohesion (Pa)	Friction angle (°)	K_c (N/m^{n+1}) *	K_ϕ (N/m^{n+2}) *	Consistency ($k=k_c+bk_\phi$)	Deformation coeff (n)**	Drawbar Pull (N)
DLR soil simulant A	4.24	188	24.8	2370	60300	8400	0.63	112.7
DLR soil simulant B	4.24	441	17.8	18773	763600	95133	1.1	155.0
VL1 drift	4.29	1600	18	1400	820000	83400	1.0	151.28
VL1 blocky	5.97	5500	30.8	1400	820000	83400	1.0	319.5
VL2 crusty-cloddy	5.22	1100	34.5	1400	820000	83400	1.0	378.8
PL drift	4.36	380	23.1	1400	820000	83400	1.0	215.2
PL cloddy	5.70	170	37	1400	820000	83400	1.0	421.45
Dry sand	5.67	1040	28	990	1528000	153790	1.1	293.2
Sandy loam	5.67	1720	29	5270	1515000	156770	0.7	298.8
Clayey soil	5.67	4140	13	13190	692200	82410	0.5	79.2
MER-B 'sandy loam'	4.24	4800	20.0	28000	7600000	788000	1.0	202.7
MER-B 'slope soil'	4.24	500	20.0	6800	210000	27800	0.8	137.2

* as there is no experimental data from VL1, VL2 and PL, we have used lunar values for those soils

** as there is no experimental data from VL1, VL2 and PL, we have assumed n=1 for those soils

Table 1. Drawbar pull for the ExoMars rover configuration on different soils

From these computations, we can determine the required drive power to ExoMars rover. Engine power is related to engine torque – the maximum torque to the wheels must be greater than the moment of all resistance forces about the centre of the wheel. The drive torque is dependent on the resistance to motion and is given by:

$$\tau = R \times \left(\frac{d}{2}\right) \qquad (12)$$

From which power is given by:

$$P = \frac{Fv}{\eta} = \tau\left(\frac{2v}{d\eta}\right) \qquad (13)$$

where η=transmission efficiency ~0.6
v=motor velocity
n=gear ratio

Rover velocity (m/h)	Power consumption (DLR Soil Simulant B)		
	Flat Terrain (W)	25° deg slope (W)	99% slip (W)
20	6.3	8.9	13.3
72	22.6	32.2	47.6
100	31.4	44.7	66.1
110	34.5	49.1	72.7

Table 2. Variation in power consumption due to variations in slope and at maximum slope (99% slip)

The primary utility for these computations is in modelling the effects of the number, width and diameter of the wheels and the effect of grouser dimensions on tractive performance. Additional effects may be taken into account including the effects of slope. The slope negotiation requirements for ExoMars were defined as long nominal traversal over all terrains of slopes of 15° or less but be capable of traversing short sandy slopes of up to 25° (this is provided by the wheel-walking mechanism whereby wheels are alternately locked to provide reaction to movement). Wheel walking capability is obtained essentially for "free" due to the requirements for deployment from the stowed configuration. Soil slopes are generally limited by the angle of repose which defines the stability of a mass of soil under its own weight which is determined by its cohesion primarily. Loose, sandy soils are limited to angles of repose under 30° due to their low cohesion but highly cohesive soils (such as clays which are expected to be present but not common on Mars) can have angles of repose up to 45°. Average power consumption was defined to be that on a 15° slope. Peak power was defined by obstacle climbing which was defined as 5 times the horizontal average value. Additional power margin is required to free the rover from blocking situations - power shots of twice the peak power. Hence, traction analysis provides the basis for determining the drive power budget, the overall power budget and the required power system sizing.

6. CONCLUSIONS

We have presented the basis for two aspects of the ExoMars rover design:

(i) rover configuration and obstacle negotiation capability

(ii) rover traction performance analysis

However, (i) requires more detailed analysis based on the chassis suspension system was required. For the chassis design, 19 rover candidate approaches were considered, most of which were discarded as not conforming to one or more aspect of the mission requirements. Legged locomotion was not considered as control and coordination of legs is considered difficult. Tracked locomotion was considered to offer the best tractive performance but they tend to suffer high power consumption (up to 65-75% dissipation), particularly during turning. Six wheels were required to provide sufficient tractive effort on all candidate soils, discarding four-wheel options. This left five candidate chassis designs, all of which are variants on the springless rocker-bogie suspension system adopted on Sojourner and the Mars Exploration Rovers [13,14]. Traction analysis is dependent on footprint, so cannot differentiate between chassis suspension designs unless they yield differences in unequal distribution of ground pressure. In fact, all chassis suspension systems are designed to provide just this – equal load distribution between all wheels. Selection of these chassis concepts were determined by 3D multi-body dynamics modelling using Cosmos/Motion™ software based on the ADAMS™ kernel which on the basis of multiple factors favoured the double rocker-bogie mechanism of Fig. 4 with a mass breakdown given in Table 3.

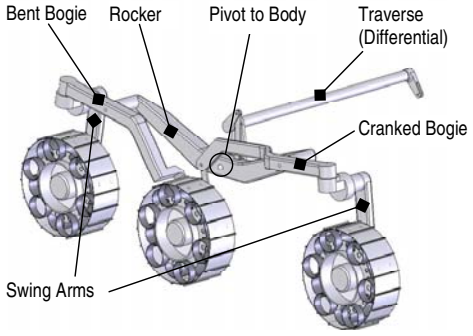

Fig. 4. Selected baseline chassis design (from EADS Astrium)

The baseline chassis design had the following mass properties:

Total rover	200 kg
Wheel with drive	6 x 4 kg
Steering mechanism with drive	4 x 2 kg
Walking mechanism drive	4 x 2.3 kg
Lever suspension system	2 x 5.8 kg
Synchronising mechanism	1 x 4 kg
Cable harness	1 x 1.4 kg
Total chassis (with 10% margin)	64 kg

Table 3. Mass breakdown of selected baseline chassis

7. REFERENCES

1. Golombek M. & Rapp D., Size-frequency distributions of rocks on Mars and Earth analogue sites: implications for future landed

missions, *J Geophysical Research* Vol. 102 (E2), 4117-4129, 1997.
2. Wilcox B. et al., Implications of statistical rock distributions on rover scaling, *Proc Intern Conf Mobile Planetary Robots & Rovers Roundup*, Santa Monica, CA, USA, 23 Jan – 1 Feb, 1997.
3. Wilcox B. et al., A nanorover for Mars, *Space Technology* Vol. 17 (3/4), 163-172, 1998.
4. Hetherington J., Applicability of the MMP concept in specifying off-road mobility for wheeled and tracked vehicles, *Journal of Terramechanics* Vol. 38, 63-70, 2001.
5. Moore H. et al., Surface materials of the Viking landing sites, *J Geophysical Research* Vol. 82 (28), 4497-4523, 1997.
6. Bekker M., *Introduction to Terrain Vehicle Systems Part 1 – The Terrain & Part 2 – The Vehicle*, University of Michigan Press, Ann Arbor, USA, 1969.
7. Bekker M., *Theory of Land Locomotion: the mechanics of vehicle mobility,* University of Michigan Press, Ann Arbor, USA, 1959.
8. Wong G., *Theory of Ground Vehicles*, 2nd Edition, John Wiley & Sons Inc, New York, USA, 2001.
9. Ellery A., Ground-Robot interaction - the basis for mobility in planetary micro-rovers*, Towards Intelligent Mobile Robots (TIMR 03), 4th British Conference on Mobile Robotics,* University of West of England, Bristol, Paper no. 8, Aug 2003.
10. Ellery A., Robot-environment interaction - the basis for mobility in planetary micro-rovers, *Robotics & Autonomous Systems* Vol. 51, 29-39, 2005.
11. Richter L. & Hamacher H., Investigating the locomotion performance of planetary microrovers with small wheel diameters and small wheel loads, *Proc 13th Intern Conf ISTVS*, Munich, Germany, 719-726, 14-17 Sept 1999.
12. Carrier W., Physical properties of the lunar surface, *Lunar Sourcebook*, ed. Heiken, G. et al., Cambridge University Press, Cambridge, UK, 522-530, 1991.
13. Patel N., Ellery A., Curley A., Sweeting M., A comparative analysis of mobility performance of planetary rover vehicles, Submitted to *ASME J Machine Design*, 2005
14. Ellery A., Richter L., Bertrand R., Chassis Design & Performance Analysis for the European ExoMars Rover*, Proc CCToMM Symposium on Mechanisms Machines & Mechatronics*, Montreal, Canada, April 2005